Global Research journal of Natural Science and Technology (Grjnst)
Volume: 02 - Issue 4 (2025)
p.ISSN: 2790-7643 e.ISSN: 2790-7651

Analytical Study of the Generalized Kudryashovs Model through the New Mapping Method with Physical Interpretation

Usman Abdul karim

Faculty of Sciences, The Superior University, Lahore, 54000 Lahore, Pakistan

abdulkarimusman256@gmail.com

Hafiza Tahira Fazal

Department of Computer Science, University of South Asia, Lahore 54000, Pakistan

tahira.fazal@usa.edu.pk

Dr. Tasadduq Niaz

Faculty of Sciences, The Superior University, Lahore, 54000 Lahore, Pakistan

tasadduq.sgd@superior.edu.pk

Abstract

The generalised Kudryashov equation, a nonlinear evolution equation that accurately simulates the propagation of ultra-short pulses in dispersive and nonlinear media, is analytically investigated in this study. A recently created generalised mapping approach is used to solve this equation. The suggested approach is more adaptable and independent of constrictive assumptions than traditional methods, which enables the derivation of a larger class of exact answers. A wide variety of soliton forms, such as W-shaped, dark, sharp, kink, peakon, bell, smooth, and anti-bell solitons, are produced using this technique. Every solution provides insightful interpretations in a range of physical circumstances and exhibits unique nonlinear behaviours impacted by the model's parameters. These solitons are important because they represent localised energy packets, intensity dips, or transitional wavefronts in domains like fluid mechanics, wave propagation, nonlinear optics, and plasma physics. The effectiveness and dependability of the novel mapping method are confirmed by the results' graphical representation, which demonstrates the generalised Kudryashov model's ability to accommodate a broad range of waveforms. Such soliton profiles' appearance highlights the

model's capacity to accurately predict intricate nonlinear processes. The study offers a clearer understanding of the rich structure of nonlinear wave events governed by higher-order dispersion and nonlinearity, in addition to improving the analytical solution space of the generalised Kudryashov equation. Combining the advanced model with the proposed mapping technique creates a robust analytical framework for studying nonlinear systems in mathematical physics and applied sciences.

Keywords: Generalized Kudryashov's Model; The New Mapping Method; Soliton Sloution; Wave profile

1 Introduction

The ability of nonlinear partial differential equations (NLPDEs) to describe a wide variety of occurrences in the natural sciences and other fields is vital. Numerous scientific and technological fields, such as fluid dynamics and the mathematical science of physics as [1], plasma physics as [2], and ecology as [3], depend heavily on NLPDEs. Several researchers have successfully built analytical travelling wave structures for non-linear partial differential equations. These findings offer significant new insights into the underlying mechanisms and have significant ramifications for our comprehension of the behaviour of complex systems. The dependable techniques that are applied to NLPDEs in order to find analytical solutions include the first integral approach [4], the inverse scattering transform scheme [5], the Weierstrass elliptic function approach [6], modified decomposition technique [7], Riccati equation scheme [8], the sine cosine approach [9], extended simplest equation approach [10], the Weierstrass elliptic function approach [11], and extended direct algebraic approach [12, 13]. Precise solutions and the study of the dynamical behaviours of optical solitons in nonlocal nonlinear media of NLPDEs are essential to understanding a range of nonlinear physical phenomena.

There are numerous techniques for obtaining precise solutions to NLPDEs, including Hirota technique [14], strategy for polynomial discriminant systems [15], modified Kudryashov's approach [16], generalized trial function technique [17], exp-expansion scheme [18, 19], sine-Gordan approach [20, 21], jacobi ansatz analysis [22], generalized variational scheme [23], exact similarity analysis [24] and Lie symmetry analysis [25, 26]. In order to investigate the interaction activities of the wave-forms, localised coordinative structures can be constructed using NLPDE solutions. Both inelastic as well as elastic impacts can occur

between localised resonances in higher dimensions, allowing two different excitations to exchange physical magnitudes like momentum and energy.

Solitons, occasionally referred to as solitary waves, can split into two solitons or merge to form a single soliton. Stable high-dimensional solitons are uncommon in nature. This is because it generally becomes challenging to achieve a balance between refraction, dispersion and nonlinearity. But in certain circumstances, highly dimensional solitons can be observed during system distribution and the nonlinear dynamics of wave packets can be well described by specific compatible nonlinear partial differential equations. For a few decades now, investigators have been studying optical solitons and other waves using each deterministic and stochastic models. Numerous findings have already been published, and the number is continuously increasing. In 2021, Kudryashov put proposed one of the most recent models to handle the dynamics of the propagation of soliton across optical fibres [27]. In this case, Generalized Kudryashov's Equation (GKE) new type is used to handle the governing model for investigating the soliton dynamics, which is the nonlinear Schrdinger's equation (NLSE) [27].

One of these models uses arbitrary power linearity to follow GKE [16].

$$i\frac{\partial Z}{\partial s}+a\frac{\partial^2 Z}{\partial r^2}+\left(\frac{\alpha_1}{(Z)^{4m}}+\frac{\alpha_2}{(Z)^{3m}}+\frac{\alpha_3}{(Z)^{2m}}+\frac{\alpha_4}{(Z)^{m}}+\alpha_5(Z)^m+\alpha_6(Z)^{2m}+\alpha_7(Z)^{3m}+\alpha_8(Z)^{4m}\right)Z=0, \quad (1.1)$$

where $Z(r,s)$ is a function having complex value, While a and α_i where $1 \le i \le 8$ are coefficients of dispersion and self phase modulation (SPM). m denotes the nonlinearity exponent parameters, where ¿ ½ $=\sqrt{-1}$. The wave profile is represented as Zï¿ ½(rï¿ ½, sï¿ ½), where s and r stand for the period and distance variables, respectively. a is linked with Dispersion of descent while α_i where $1 \le i \le 8$ are attach with self phase modulation. In [28], Eq. (1.1) was put forth and resolved. In [28], a dark, bright and smooth soliton solutions are produced when α_2= α_4= α_5=α_7= 0. In [29], Jacobi's elliptic expansion tecnique is used to solve equation Eq. (1.1) where m=1, α_2= α_3= α_4= α_5= α_7= 0. Eq. (1.1) is examined in [30] when $\alpha_1 = \alpha_2 = \alpha_7 = \alpha_8$=0 utilising the Painleve methodology and the exponential rational function approach. We find several novel soliton solutions for equation Eq. (1.1) in this work. Certain soliton solutions will be brilliant, dark, and kink when $\alpha_1 = \alpha_2$=0, whereas other soliton solutions will be bright and dark when α_7=α_8= 0. Here, we explore

the generalised Kudryashov model, a complex nonlinear evolution equation that adds higher-order dispersive and nonlinear effects to the classical Kudryashov framework. This generalisation improves the model's ability to more accurately predict the propagation of ultra-short optical pulses in nonlinear and dispersive environments.

The concept is especially applicable to photonic systems, fibre optics, and nonlinear transmission lines, where waveforms change as a result of intricate interactions between dispersion, nonlinearity, and any outside disturbances. We provide a recently suggested generalised mapping method that systematically converts the partial differential equation (PDE) to an ordinary differential equation (ODE) using an advanced variable transformation and an appropriate ansatz in order to extract analytical solutions from this complex model. The proposed mapping method does not rely on limiting solution forms or standard balancing principles like traditional methods do. Rather, it makes use of an adaptable algebraic transformation structure that expands the range of possible solutions. Depending on the parametric regimes and nonlinear coefficients involved, this novel method enables us to create a rich family of exact solutions, including kink-type waves, bright solitons, dark solitons, and other localised waveforms. The approach demonstrates flexibility and efficiency while providing a deeper understanding of how nonlinear parameters influence wave behaviour. Its potential as a general-purpose tool for solving a broad class of nonlinear PDEs in mathematical physics is demonstrated by the analytical findings obtained, which validate the mapping strategy's consistency and resilience. All things considered, this new mapping method in conjunction with the generalised Kudryashov model greatly improves our comprehension of nonlinear wave mechanics and expands the analytical toolkit for examining soliton dynamics in complicated media.

The distribution of the remaining paper is listed below: Section 2 provides the overview of suggested method. Section 3 containing the application of suggested approach , section 4 containing the physically interpretation and application of above results, section 5 containing the stability analysis, section 6 containing the physical interpretation while comparison is in section 7 and Section 8 contain the conclusion and future research .

2 Description of the Methodology

The description of the analytical methodology is included in this section. let assume the NLPDE

$$N(Z, Z_r, Z_s, Z_{rr}, Z_{ss}, Z_{rs} \ldots\ldots\ldots) = 0, \tag{2.1}$$

where in above Eq. (2.1) $Z(r,s)$ is a function that is unknow. To solve the Eq. (1.1) we use the wave transformation is in the following form

$$Z(r,s) = W(q)e^{\iota\phi}, \quad q = \beta r - \eta s, \quad \phi = -\xi r + \varphi s + \rho. \tag{2.2}$$

where W(q) is a function takin real value, while η, ϵ and φ are constants. The soliton wave's frequency is represented by ξ, its rate of acceleration by η, its intensity component by W(q) and its modulation number by φ.

Eq. (2.1) reduce to an ODE

$$O(Y, Y', Y'', Y''', \ldots\ldots\ldots) = 0. \tag{2.3}$$

Our methodology strategy is discussed in following steps,

Step 1. Ensuring use of limitations,

$$W(q) = Y^{\frac{1}{2m}}(q), \quad Y(q) > 0, \tag{2.4}$$

Y(q) is the hold the solution is of the form,

$$Y(q) = \tau_0 + \tau_1 B(q) + \tau_2 B(q)^2, \quad \tau_2 \neq 0, \tag{2.5}$$

provided that B(q) is governed by the associated ancillary equation is of the form,

$$(B'(q))^2 = b_1 + b_2 B(q)^2 + \frac{1}{2} b_3 B(q)^4 + \frac{1}{3} b_4 B(q)^6. \tag{2.6}$$

Where b_1,b_2,b_3,b_4 and τ_0, τ_1, τ_2 are constants.

Step 2. We use the balancing strategy to compare the non linear terms .

Step 3. Substituting Eq. (2.5) and Eq. (2.6) in Eq. (2.3) and by setting parameters of $B^n(q)$ equal to zero , we acquire a set of algebraic equations. The Mathematica software can be used to solve the algebraic set of equation that we drive.

Step 4. By combining the solutions of Eq. (2.3) with Eq. (2.2) , several analytical solutions of Eq. (2.1) can be found.

Solution to Eq. (2.6) mention as:

Case 1. With the help of $b_1 = \frac{16\, b_2^2}{27\, b_3}$, and $b_4 = \frac{3\, b_3^2}{16\, b_2}$, the exact solution of Eq. (2.6) is of the form ;

$$B_1(q) = 4\sqrt{\frac{-b_2 \tanh^2\left(\delta\sqrt{\frac{-b_2}{3}}\, q\right)}{3\, b_3\left(3+\tanh^2\left(\delta\sqrt{\frac{-b_2}{3}}\, q\right)\right)}}, \quad b_2 < 0, \;\; b_3 > 0, \tag{2.7}$$

$$B_2(q) = 4\sqrt{\frac{-b_2 \coth^2\left(\delta\sqrt{\frac{-b_2}{3}}\, q\right)}{3\, b_3\left(3+\coth^2\left(\delta\sqrt{\frac{-b_2}{3}}\, q\right)\right)}}, \quad b_2 < 0, \;\; b_3 > 0. \tag{2.8}$$

$$B_3(q) = 4\sqrt{\frac{b_2 \tan^2\left(\delta\sqrt{\frac{b_2}{3}}\, q\right)}{3\, b_3\left(3-\tan^2\left(\delta\sqrt{\frac{b_2}{3}}\, q\right)\right)}}, \quad b_2 > 0, \;\; b_3 < 0, \tag{2.9}$$

$$B_4(q) = 4\sqrt{\frac{b_2 \cot^2\left(\delta\sqrt{\frac{b_2}{3}}\, q\right)}{3\, b_3\left(3-\cot^2\left(\delta\sqrt{\frac{b_2}{3}}\, q\right)\right)}}, \quad b_2 > 0, \;\; b_3 < 0. \tag{2.10}$$

Case 2. With the help of $b_1 = 0$, and $b_4 = \frac{3\, b_3^2}{16\, b_2}$ the exact solution of Eq. (2.6) is of the form;

$$B_5(q) = \sqrt{\frac{-2b_2}{b_3}\left(1 + \tanh\left(\delta\sqrt{b_2}\, q\right)\right)}, \quad b_2 > 0, \tag{2.11}$$

and

$$B_6(q) = \sqrt{\frac{-2b_2}{b_3}\left(1 + \coth\left(\delta\sqrt{b_2}\, q\right)\right)}, \quad b_2 > 0, \tag{2.12}$$

Case 3. With the help of $b_1 = 0$, the exact solution of Eq. (2.6) is of the form ;

$$B_7(q) = \sqrt{-\frac{6\, b_2\, b_3\, sech^2\left(\sqrt{b_2}\, q\right)}{3b_3^2 - 4b_2 b_4\left(1+\delta\, \tanh\left(\sqrt{b_2}\, q\right)\right)^2}}, \quad b_2 > 0, \tag{2.13}$$

or

$$B_8(q) = \sqrt{\frac{6\, b_2\, b_3\, csch^2\left(\sqrt{b_2}\, q\right)}{3b_3^2 - 4b_2 b_4\left(1+\delta\, \coth\left(\sqrt{b_2}\, q\right)\right)^2}}, \quad b_2 > 0. \tag{2.14}$$

and

$$B_9(q) = \sqrt{-\frac{6\, b_2\, sech^2\left(\sqrt{b_2}\, q\right)}{3b_3 + 4\delta\sqrt{3b_2 b_4}\, \tanh\left(\sqrt{b_2}\, q\right)}}, \quad b_2 > 0, \;\; b_4 > 0, \tag{2.15}$$

or

$$B_{10}(q) = \sqrt{\frac{6b_2, csch^2\left(\sqrt{b_2}\, q\right)}{3b_3 + 4\delta\sqrt{3b_2 b_4}\, \coth\left(\sqrt{b_2}\, q\right)}} \quad b_2 > 0, \;\; b_4 > 0, \tag{2.16}$$

where $\delta = \pm 1$.

3 Application of New mapping Method

After substituting Eq. (2.2) in Eq. (1.1) and by setting equal to zero we obtain a real and imaginary parts as follows:

$$a\beta^2 W''(q) + (-a\xi^2 - \varphi)W(q) + \alpha_1 W(q)^{1-4m} + \alpha_2 W(q)^{1-3m} + \alpha_3 W(q)^{1-2m} + \alpha_4 W(q)^{1-m} + \alpha_5 W(q)^{1+m} + \alpha_6 W(q)^{1+2m} + \alpha_7 W(q)^{1+3m} + \alpha_8 W(q)^{1+4m} = 0, \tag{3.1}$$

and

$$\eta = -2a\beta\xi \tag{3.2}$$

Ensuring the uses of limitation as given in Eq. (2.4) in to Eq. (3.1) then we obtain,

$$a\beta^2(1-2m)\left(\frac{dY(q)}{dq}\right)^2 + 2m\,a\beta^2\,Y(q)\frac{d^2Y(q)}{dq^2} + 4m^2\alpha_1 + 4m^2\alpha_2 Y(q)^{\frac{1}{2}} + 4m^2\alpha_3\,Y(q)$$
$$+4m^2(-a\xi^2-\varphi)\,Y(q)^2 + 4m^2\alpha_4 Y(q)^{\frac{3}{2}} + 4m^2\alpha_5 Y(q)^{\frac{5}{2}} + 4m^2\alpha_7 Y(q)^{\frac{7}{2}} + 4m^2\alpha_6\,Y(q)^3 + 4m^2\alpha_8\,Y(q)^4 =$$

(3.3)

We use specific criteria to secure the analytical solution,

$$\alpha_2 = 0,\ \alpha_4 = 0,\ \alpha_5 = 0,\ \alpha_7 = 0. \tag{3.4}$$

Then equation Eq. (3.3) reduced to

$$a\beta^2(1-2m)\left(\frac{dY(q)}{dq}\right)^2 + 2m\,a\beta^2\,Y(q)\frac{d^2Y(q)}{dq^2} + 4m^2\alpha_1 + 4m^2\alpha_3\,Y(q)$$
$$+4m^2(-a\xi^2-\varphi)\,Y(q)^2 + 4m^2\alpha_6\,Y(q)^3 + 4m^2\alpha_8\,Y(q)^4 = 0. \tag{3.5}$$

Balancing $Y(q)Y''(q)$ and $(Y(q))^4$ in Eq. (3.5) we obtain the balance number N=1. Thus the Eq. (2.5) is analytical solution for Eq. (3.5) as

$$(B'(q))^2 = b_1 + b_2B(q)^2 + \frac{1}{2}b_3B(q)^4 + \frac{1}{3}b_4B(q)^6. \tag{3.6}$$

Substitute Eq. (3.6) along with Eq. (2.6) in Eq. (3.5) we obtain a system of algebraic equations

$$\begin{cases} B^8(q) = \frac{4}{3}a\beta^2 b_4\tau_2^2 + \frac{8}{3}am\beta^2 b_4\tau_2^2 + 4m^2\alpha_8\tau_2^4 = 0, \\ B^7(q) = \frac{4}{3}a\beta^2 b_4\tau_1\tau_2 + \frac{14}{3}am\beta^2 b_4\tau_1\tau_2 + 16m^2\alpha_8\tau_1\tau_2^3 = 0, \\ B^6(q) = \frac{1}{3}a\beta^2 b_4\tau_1^2 + \frac{4}{3}am\beta^2 b_4\tau_1^2 + \frac{16}{3}am\beta^2 b_4\tau_0\tau_2 + 2a\beta^2 b_3\tau_2^2 + 2am\beta^2 b_3\tau_2^2 \\ +24m^2\alpha_8\tau_1^2\tau_2^2 + 4m^2\alpha_6\tau_2^3 + 16m^2\alpha_8\tau_0\tau_2^3 = 0, \\ B^5(q) = 2am\beta^2 b_4\tau_0\tau_1 + 2a\beta^2 b_3\tau_1\tau_2 + 4am\beta^2 b_3\tau_1\tau_2 + 16m^2\alpha_8\tau_1^3\tau_2 + 12m^2\alpha_6\tau_1\tau_2^2 + 48m^2\alpha_8\tau_0\tau_1\tau_2^2 = \\ B^4(q) = \frac{1}{2}a\beta^2 b_3\tau_1^2 + am\beta^2 b_3\tau_1^2 + 4m^2\alpha_8\tau_1^4 + 6am\beta^2 b_3\tau_0\tau_2 + 12m^2\alpha_6\tau_1^2\tau_2 + 48m^2\alpha_8\tau_0\tau_1^2\tau_2 \\ -4am^2\xi^2\tau_2^2 - 4m^2\phi\tau_2^2 + 4a\beta^2 b_2\tau_2^2 + 12m^2\alpha_6\tau_0\tau_2^2 + 24m^2\alpha_8\tau_0^2\tau_2^2 = 0, \\ B^3(q) = 2am\beta^2 b_3\tau_0\tau_1 + 4m^2\alpha_6\tau_1^3 + 16m^2\alpha_8\tau_0\tau_1^3 - 8am^2\xi^2\tau_1\tau_2 - 8m^2\phi\tau_1\tau_2 + 4a\beta^2 b_2\tau_1\tau_2 \\ +2am\beta^2 b_2\tau_1\tau_2 + 24m^2\alpha_6\tau_0\tau_1\tau_2 + 48m^2\alpha_8\tau_0^2\tau_1\tau_2 = 0, \\ B^2(q) = -4am^2\xi^2\tau_1^2 - 4m^2\phi\tau_1^2 + a\beta^2 b_2\tau_1^2 + 12m^2\alpha_6\tau_0\tau_1^2 + 24m^2\alpha_8\tau_0^2\tau_1^2 + 4m^2\alpha_3\tau_2 - 8am^2\xi^2\tau_0\tau_2 \\ -8m^2\phi\tau_0\tau_2 + 8am\beta^2 b_2\tau_0\tau_2 + 12m^2\alpha_6\tau_0^2\tau_2 + 16m^2\alpha_8\tau_0^3\tau_2 + 4a\beta^2 b_1\tau_2^2 - 4am\beta^2 b_1\tau_2^2 = 0, \\ B^1(q) = 4m^2\alpha_3\tau_1 - 8am^2\xi^2\tau_0\tau_1 - 8m^2\phi\tau_0\tau_1 + 2am\beta^2 b_2\tau_0\tau_1 + 12m^2\alpha_6\tau_0^2\tau_1 + 16m^2\alpha_8\tau_0^3\tau_1 + 4a\beta^2 b_1\tau \\ -4am\beta^2 b_1\tau_1\tau_2 = 0, \\ B^0(q) = 4m^2\alpha_1 + 4m^2\alpha_3\tau_0 - 4am^2\xi^2\tau_0^2 - 4m^2\phi\tau_0^2 + 4m^2\alpha_6\tau_0^3 + 4m^2\alpha_8\tau_0^4 = 0. \end{cases}$$

(3.7)

Solve this system we obtain,

Case 1. With the help of $b_1 = \frac{16\,b_2^2}{27\,b_3}$, and $b_4 = \frac{3\,b_3^2}{16\,b_2}$, then Eq. (3.7) gives,

$$\begin{cases} \tau_0 = \tau_0,\ \tau_1 = 0,\ \tau_2 = 2\tau_0,\ b_3 = b_3, \\ b_2 = \frac{3\,b_3^2\,\beta^2}{32\,m^2\,\alpha_8\,\tau_2},\ \alpha_3 \neq 0,\ \alpha_6 \neq 0, \\ \varphi = \frac{2\,\alpha_8\,(\tau_2)^3}{\tau_0}, \end{cases} \tag{3.8}$$

Substitute Eq. (3.8) together with (2.7) to (2.10) in Eq. (2.5) we obtain,

$$Z_1(r,s) = \left[\tau_0\left(1 - \frac{8b_2}{9b_3^2\sinh^2\left(2\delta\sqrt{-\frac{b_2}{3}}(\beta r - \eta s)\right)}\right)\right]^{\frac{1}{2m}} \cdot e^{i(-\xi r + \varphi s + \rho)}, \tag{3.9}$$

$$Z_2(r,s)=\left[\tau_0\left(1-\frac{8b_2}{9b_3^2\cosh^2\left(2\delta\sqrt{-\frac{b_2}{3}}(\beta r-\eta s)\right)}\right)\right]^{\frac{1}{2m}}\cdot e^{i(-\xi r+\varphi s+\rho)}, \quad (3.10)$$

$$Z_3(r,s)=\left[\tau_0\left(1+\frac{32b_2}{9b_3^2}\cdot\frac{\left(1-\cos^2\left(\delta\sqrt{\frac{b_2}{3}}(\beta r-\eta s)\right)\right)^2}{\left(4\cos^2\left(\delta\sqrt{\frac{b_2}{3}}(\beta r-\eta s)\right)-1\right)^2}\right)\right]^{\frac{1}{2m}}\cdot e^{i(-\xi r+\varphi s+\rho)}, \quad (3.11)$$

$$Z_4(r,s)=\left[\tau_0\left(1+\frac{32b_2}{9b_3^2}\cdot\frac{\left(1-\sin^2\left(\delta\sqrt{\frac{b_2}{3}}(\beta r-\eta s)\right)\right)^2}{\left(2\sin^2\left(\delta\sqrt{\frac{b_2}{3}}(\beta r-\eta s)\right)+1\right)^2}\right)\right]^{\frac{1}{2m}}\cdot e^{i(-\xi r+\varphi s+\rho)}. \quad (3.12)$$

Case 2. With the help of $b_1=0$ and $b_4=\frac{3\,b_3^2}{16\,b_2}$, then Eq. (3.7) gives,

$$\begin{cases}\tau_0=\tau_0,\ \tau_1=0,\ \tau_2=2\tau_0,\ b_3=b_3,\\ b_2=\frac{3\,b_3^2\,\beta^2}{128\,m^2\,\alpha_8\,\tau_0^2},\ \alpha_3\neq 0,\ \alpha_6\neq 0,\\ \varphi=16\,\alpha_8\,\tau_0^2,\end{cases} \quad (3.13)$$

Substitute Eq. (3.13) together with (2.11) and (2.12) in Eq. (2.5) we obtain,

$$Z_5(r,s)=\left[\tau_0\left(1-\frac{3b_3\beta^2}{32m^2\alpha_8\tau_0^2}\left(1+\tanh\left(\delta\sqrt{b_2}\cdot(\beta r-\eta s)\right)\right)^2\right)\right]^{\frac{1}{2m}}\cdot e^{i(-\xi r+\varphi s+\rho)}, \quad (3.14)$$

$$Z_6(r,s)=\left[\tau_0\left(1-\frac{3b_3\beta^2}{32m^2\alpha_8\tau_0^2}\left(1+\coth\left(\delta\sqrt{b_2}\cdot(\beta r-\eta s)\right)\right)^2\right)\right]^{\frac{1}{2m}}\cdot e^{i(-\xi r+\varphi s+\rho)}. \quad (3.15)$$

Case 3. With the help of $b_1 = 0$ then Eq. (3.7) gives,

$$\begin{cases} \tau_0 = \tau_0,\ \tau_1 = 0,\ \tau_2 = 2\tau_0,\ b_3 = b_3, \\ b_2 = \frac{3\, b_3^2\, \beta^2}{128\, m^2\, \alpha_8\, \tau_0^2},\ b_4 = \frac{8\, m^2\, \alpha_8\, \tau_0^2}{\beta^2},\ \alpha_3 \neq 0,\ \alpha_6 \neq 0, \\ \varphi = 16\, \alpha_8\, \tau_0^2, \end{cases} \tag{3.16}$$

Substitute Eq. (3.16) together with (2.13) to (2.16) in Eq. (2.5) we obtain,

$$Z_7(r,s) = \left[\tau_0\left(1 - \frac{12 b_2 b_3}{\cosh^2\left(\sqrt{b_2}q\right)\left(3b_3^2 - 4b_2 b_4\left(1+\delta\frac{\sinh\left(\sqrt{b_2}q\right)}{\cosh\left(\sqrt{b_2}q\right)}\right)^2\right)}\right)\right]^{\frac{1}{2m}} \cdot$$

$e^{i(-\xi r+\varphi s+\rho)}$, (3.17)

$$Z_8(r,s) = \left[\tau_0\left(1 + \frac{12 b_2 b_3}{\sinh^2\left(\sqrt{b_2}q\right)\left(3b_3^2 - 4b_2 b_4\left(1+\delta\frac{\cosh\left(\sqrt{b_2}q\right)}{\sinh\left(\sqrt{b_2}q\right)}\right)^2\right)}\right)\right]^{\frac{1}{2m}} \cdot$$

$e^{i(-\xi r+\varphi s+\rho)}$, (3.18)

$$Z_9(r,s) = \left[\tau_0\left(1 - \frac{12 b_2}{\cosh^2\left(\sqrt{b_2}q\right)\left(3b_3 + 4\delta\sqrt{3b_2 b_4}\cdot\frac{\sinh\left(\sqrt{b_2}q\right)}{\cosh\left(\sqrt{b_2}q\right)}\right)}\right)\right]^{\frac{1}{2m}} \cdot e^{i(-\xi r+\varphi s+\rho)}, \tag{3.19}$$

$$Z_{10}(r,s) = \left[\tau_0\left(1 + \frac{12 b_2}{\sinh^2\left(\sqrt{b_2}q\right)\left(3b_3 + 4\delta\sqrt{3b_2 b_4}\cdot\frac{\cosh\left(\sqrt{b_2}q\right)}{\sinh\left(\sqrt{b_2}q\right)}\right)}\right)\right]^{\frac{1}{2m}} \cdot$$

$e^{i(-\xi r+\varphi s+\rho)}$. (3.20)

4 Graphical Findings and discussion

In this study, we used the new Mapping technique to analytically solve the NLSE using generalized Kudryashov's equation. These solutions are obtained through the application of this persuasive method. The proposed method successfully yields the analytical solutions for the nonlinear GKEÂ in paired vector shape in birefringent fibre without four-wave mixing. Several analytic solutions for GKE are generated using suggested approach. The findings provide insight into a number of novel wave patterns that aid in illuminating the GKE. The results demonstrate the utility of the proposed approach as it may provide a range of innovative analytical solutions for particular nonlinear real-world models.

This section explains the results' visual representations using both 2D and 3D graphs. When the GKE is implemented, solitary waves of various shapes, including W, dark, sharp, kink, peakon, bell, smooth, and anti-bell types, can be produced using the previously described technique. A wide range of soliton structures, each representing unique nonlinear wave behaviours, are depicted in the graphical results: W-shaped, dark, sharp, kink, peakon, bell, smooth, and anti-bell. Realistic scientific events including shock waves, fluid dynamics, and optical pulses are depicted in these profiles. Their appearance demonstrates how well the generalised Kudryashov model captures intricate soliton dynamics and how reliable the novel mapping technique is.

Considering parametric variables to take into consideration for the hyperbolic solution in $Z_1(r,s)$, we derive the dark wave soliton solution for the 3D and 2D plots with $\tau_0 = -10$, $m = 0.05$, $\alpha_6 = 1.5$, $\alpha_8 = 0.01$, $a = -1.005$, $\beta = 0.4$, $\delta = 1$, $b_3 = 0.6$,$\xi = 1.03$ and $\rho = 5.36$. as shown in Figure 1. Considering parametric variables to take into consideration for hyperbolic solution in $Z_2(r,s)$, we derive the Â W shape wave soliton solution for the 3D and 2D plots with$\tau_0 = 5$, $m = 5.02$, $\alpha_6 = 5$, $\alpha_8 = 0.2$, $a = -0.1$, $\beta = 0.4$, $\delta = -1$, $b_3 = -0.6$,$\xi = 2$ and $\rho = -0.1$. as shown in Figure 2. Considering parametric variables to take into consideration for the trigonometric solution in $Z_3(r,s)$, we derive the Â peakon wave soliton solution for the 3D and 2D plots with $\tau_0 = -10$, $m = -1.2$, $\alpha_8 = -0.02$, $a = -0.2$, $\beta = 4$, $\delta = 1$, $b_3 = 1.6$,$\xi = -2.6$ and $\rho = 5$. as shown in Figure 3. Considering parametric variables to take into consideration for the trigonometric solution in $Z_4(r,s)$, we derive the solitary wave soliton solution for the 3D and 2D plots with $\tau_0 = 10$, $m = 0.02$, $\alpha_8 = -0.2$, $a = 0.02$, $\beta =$

-0.4, $\delta = -1$, $b_3 = 1.6$,$\xi = -1$ and $\rho = -5$. as shown in Figure 4. Considering parametric variables to take into consideration for the hyperbolic solution in $Z_5(r,s)$, we derive the kink soliton solution for the 3D and 2D plots with $\tau_0 = 2.05$, $m = 1.2$, $\alpha_8 = 1$, $a = 0.2$, $\beta = 4$, $\delta = -1$, $b_3 = 1.6$,$\xi = -2.6$ and $\rho = 5$. as shown in Figure 5. Considering parametric variables to take into consideration for the hyperbolic solution in $Z_6(r,s)$, we derive the peakon type wave soliton solution for the 3D and 2D plots with $\tau_0 = 5$, $m = 2.2$, $\alpha_8 = 2$, $a = 0.1$, $\beta = 3$, $\delta = -1$, $b_3 = 1.6$,$\xi = -2.6$ and $\rho = -5$ as shown in Figure 6. Considering parametric variables to take into consideration for the hyperbolic solution in $Z_7(r,s)$, we derive the Â anti bell wave soliton solution for the 3D and 2D plots with $\tau_0 = -10$, $m = 12$, $\alpha_8 = 1.3$, $a = -0.6$, $\beta = 10$, $\delta = -1$, $b_3 = 0.33$,$\xi = -2$ and $\rho = -1$. as shown in Figure 7. Considering parametric variables to take into consideration for the hyperbolic solution in $Z_8(r,s)$, we derive the Â dark wave solitons solution for the 3D and 2D plots with $\tau_0 = -10$, $m = -0.05$, $\alpha_6 = 1.5$, $\alpha_8 = -0.1$, $a = 1.5$, $\beta = -0.4$, $\delta = -1$, $b_3 = 0.6$,$\xi = 1.03$ and $\rho = 5.36$ as shown in Figure 8. Considering parametric variables to take into consideration for the hyperbolic function solution in $Z_9(r,s)$, we derive the Â bright wave soliton solution for the 3D and 2D plots with $\tau_0 = 10$, $m = 0.05$, $\alpha_6 = 1.5$, $\alpha_8 = -0.1$, $a = 1.5$, $\beta = -0.4$, $\delta = -1$, $b_3 = 0.6$,$\xi = 1.03$ and $\rho = 5.36$ as shown in Figure 9. Considering parametric variables to take into consideration for the hyperbolic function solution in $Z_{10}(r,s)$, we derive the anti peakon wave soliton solution for the 3D and 2D plots with $\tau_0 = -10$, $m = -2.05$, $\alpha_6 = 1.5$, $\alpha_8 = -0.1$, $a = 1.05$, $\beta = -0.4$, $\delta = 1$, $b_3 = 0.6$,$\xi = -1.54$ and $\rho = 5.36$ as shown in Figure 10.

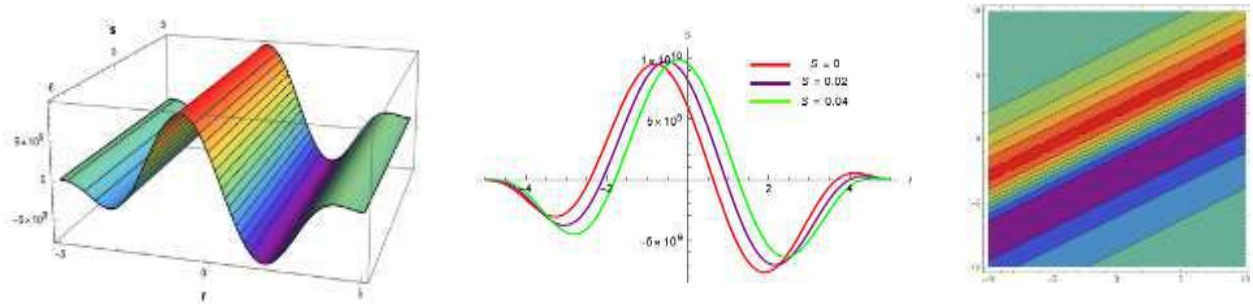

(a) 3D Plot (b) 2D Plot (c) Contour Plot

Figure 1: Solution for Eq. (3.9) gives dark wave solution profile for $\tau_0 = -10$, $m = 0.05$, $\alpha_6 = 1.5$, $\alpha_8 = 0.01$, $a = -1.005$, $\beta = 0.4$, $\delta = 1$, $b_3 = 0.6$,$\xi = 1.03$ and $\rho = 5.36$

(a): 3D plot, (b): 2D plot, (c): contour plot

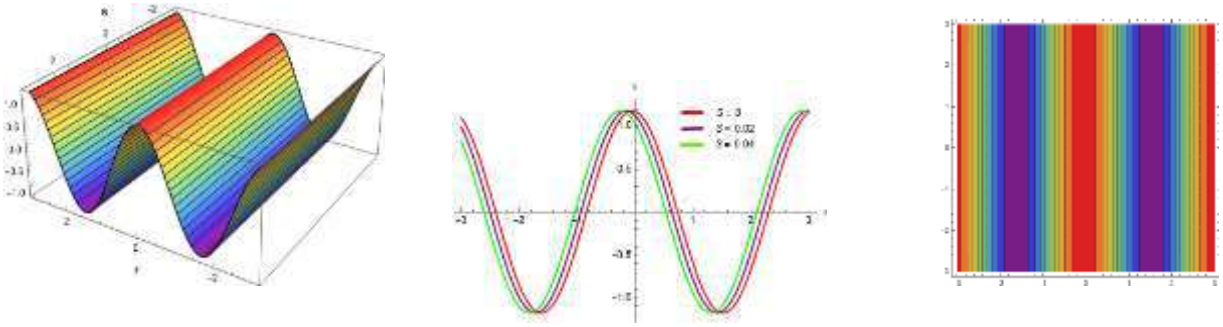

(a) 3D Plot (b) 2D Plot (c) Contour Plot

Figure 2: Solution for Eq. (3.10) gives a W shape wave soliton solution profile for $\tau_0 = 5$, $m = 5.02$, $\alpha_6 = 5$, $\alpha_8 = 0.2$, $a = -0.1$, $\beta = 0.4$, $\delta = -1$, $b_3 = -0.6$,$\xi = 2$ and $\rho = -0.1$

(a): 3D plot, (b): 2D plot, (c): contour plot

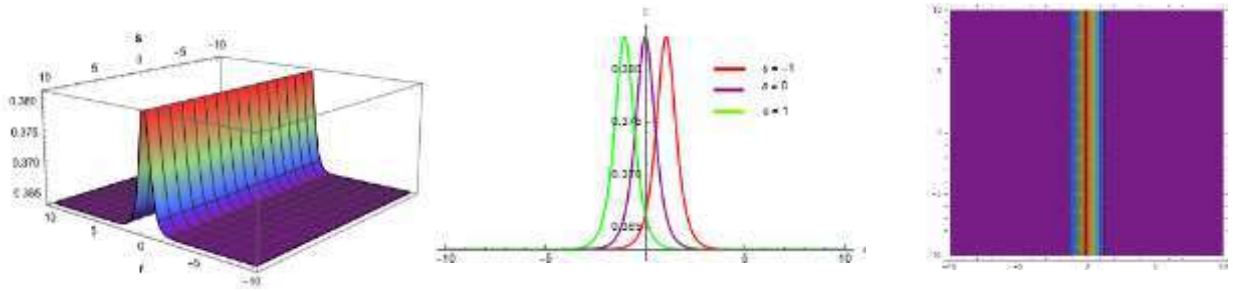

(a) 3D Plot (b) 2D Plot (c) Contour Plot

Figure 3: Solution for Eq. (3.11) gives a bell or peakon wave soliton solution profile for $\tau_0 = -10$, $m = -1.2$, $\alpha_8 = -0.02$, $a = -0.2$, $\beta = 4$, $\delta = 1$, $b_3 = 1.6$,$\xi = -2.6$ and $\rho = 5$ .4-15;

a: 3D plot 4-15b:2D plot 4-14c: contour plot

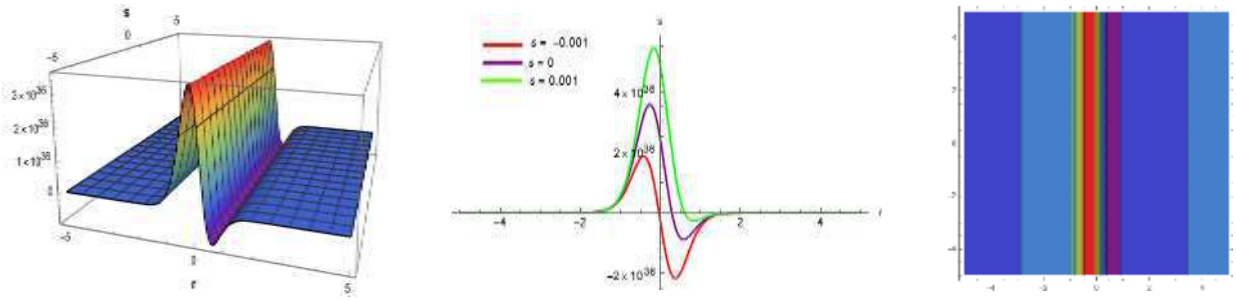

(a) 3D Plot (b) 2D Plot (c) Contour Plot

Figure 4: Solution for Eq. (3.12) gives a dark wave soliton solution profile for $\tau_0 = 10$, $m = 0.02$, $\alpha_8 = -0.2$, $a = 0.02$, $\beta = -0.4$, $\delta = -1$, $b_3 = 1.6$,$\xi = -1$ and $\rho = -5$

(a): 3D plot, (b): 2D plot, (c): contour plot

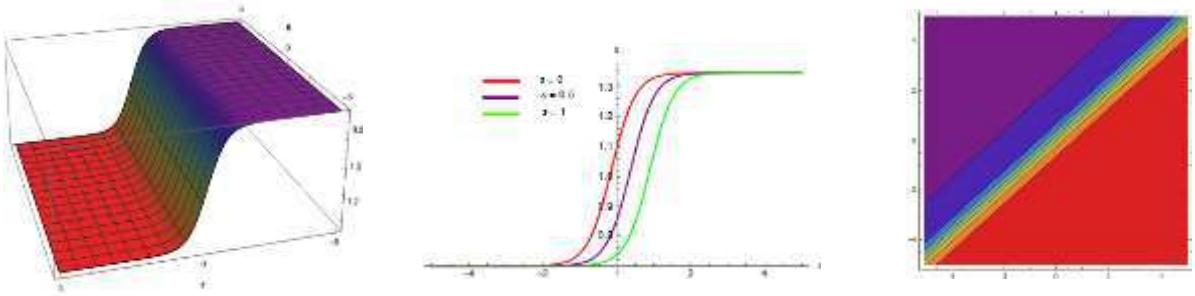

(a) 3D Plot (b) 2D Plot (c) Contour Plot

Figure 5: Solution for Eq. (3.14) give kink soliton solution profile for $\tau_0 = 2.05$, $m = 1.2$, $\alpha_8 = 1$, $a = 0.2$, $\beta = 4$, $\delta = -1$, $b_3 = 1.6$,$\xi = -2.6$ and $\rho = 5$

(a): 3D plot, (b): 2D plot, (c): contour plot

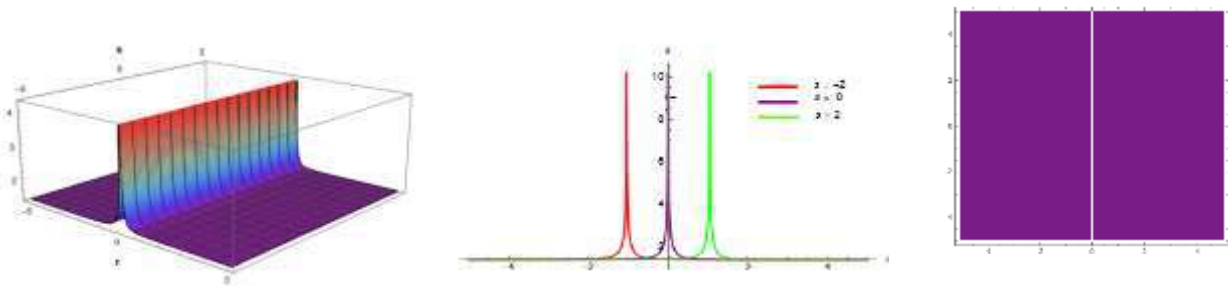

(a) 3D Plot (b) 2D Plot (c) Contour Plot

Figure 6: Solution for Eq. (3.15) gives a Peakon wave soliton solution profile for $\tau_0 = 5$, $m = 2.2$, $\alpha_8 = 2$, $a = 0.1$, $\beta = 3$, $\delta = -1$, $b_3 = 1.6$,$\xi = -2.6$ and $\rho = -5$

(a): 3D plot, (b): 2D plot, (c): contour plot

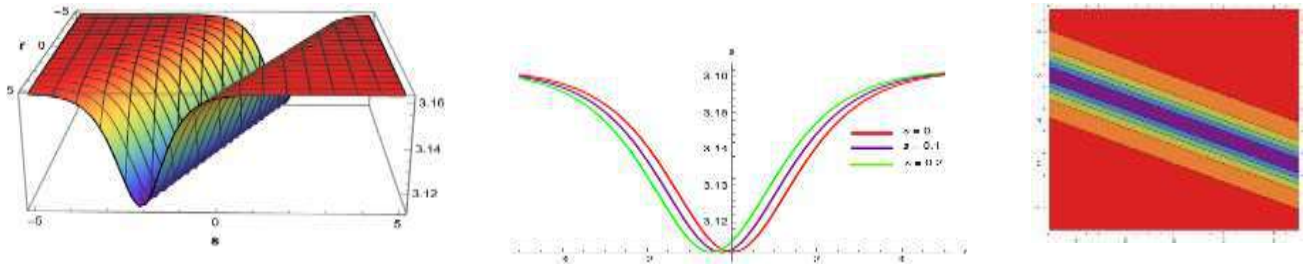

(a) 3D Plot (b) 2D Plot (c) Contour Plot

Figure 7: Solution for Eq. (3.17) gives a anti bell wave soliton solution profile for $\tau_0 = -10, m = 12, \alpha_8 = 1.3, a = -0.6, \beta = 10, \delta = -1, b_3 = 0.33, \xi = -2$ and $\rho = -1$

(a): 3D plot, (b): 2D plot, (c): contour plot

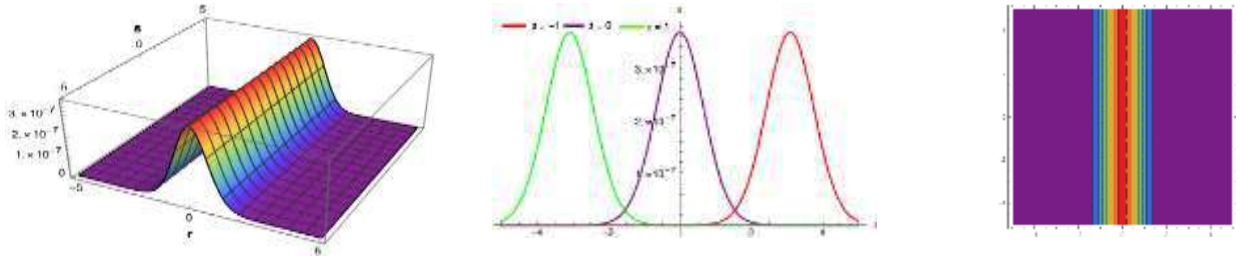

(a) 3D Plot (b) 2D Plot (c) Contour Plot

Figure 8: Solution for Eq. (3.18) gives a bright wave type soliton solution profile for $\tau_0 = -10, m = -0.05, \alpha_6 = 1.5, \alpha_8 = -0.1, a = 1.5, \beta = -0.4, \delta = -1, b_3 = 0.6, \xi = 1.03$ and $\rho = 5.36$; (a): 3D plot, (b): 2D plot, (c): contour plot

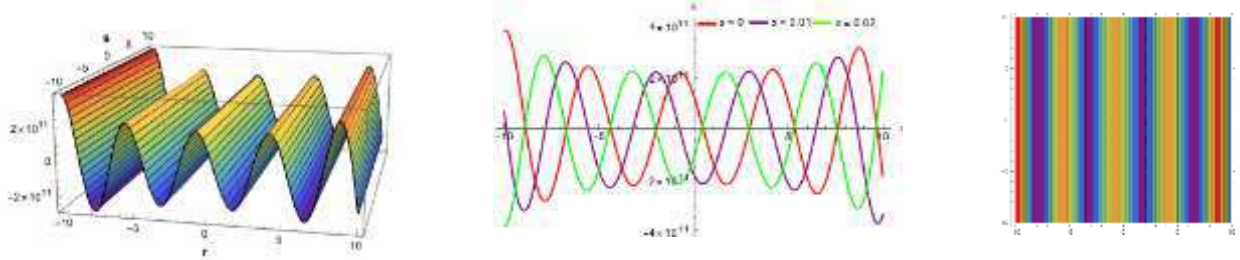

(a) 3D Plot (b) 2D Plot (c) Contour Plot

Figure 9: Solution for Eq. (3.19) gives priodic wave soliton solution profile for $\tau_0 = 10, m = 0.05, \alpha_6 = 1.5, \alpha_8 = -0.1, a = 1.5, \beta = -0.4, \delta = -1, b_3 = 0.6, \xi = 1.03$ and $\rho = 5.36$ (a): 3D plot, (b): 2D plot, (c): contour plot

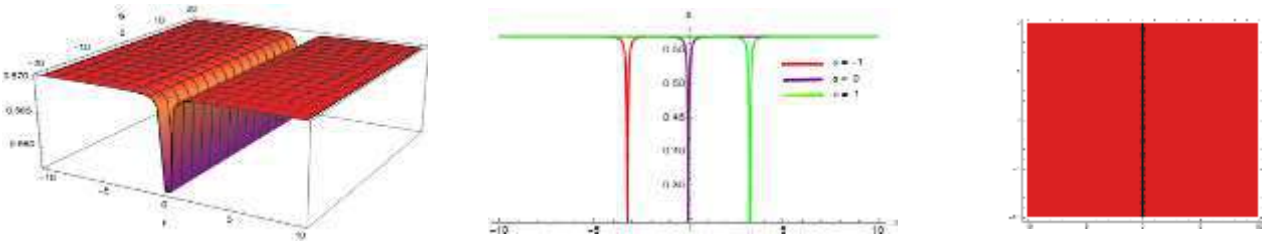

(a) 3D Plot (b) 2D Plot (c) Contour Plot

Figure 10: Solution for Eq. (3.20) gives a anti peakon wave soliton solution profile for $\tau_0 = -10$, $m = -2.05$, $\alpha_6 = 1.5$, $\alpha_8 = -0.1$, $a = 1.05$, $\beta = -0.4$, $\delta = 1$, $b_3 = 0.6$,$\xi = -1.54$ and $\rho = 5.36$; (a): 3D plot, (b): 2D plot, (c): contour plot

5 Stability Analysis

This section will examine the stability analysis [31] for GKE. Suppose that the perturbation solution has the following form of (1.1).

$$Z(r,s) = \beta\eta(r,s) + \mu_0. \tag{5.1}$$

It is evident that any constant μ_0 constitutes a steady-state solution for equation (1.1). Substitute (5.1) in (1.1) we obtain

$$\iota\beta\eta_s + a\beta\eta_{rr} + \Lambda(\beta\eta + \mu_0) = 0. \tag{5.2}$$

Where $\Lambda = (\frac{\alpha_1}{(\beta\eta(r,s)+\mu_0)^{4m}} + \frac{\alpha_2}{(\beta\eta(r,s)+\mu_0)^{3m}} + \frac{\alpha_3}{(\beta\eta(r,s)+\mu_0)^{2m}} + \frac{\alpha_4}{(\beta\eta(r,s)+\mu_0)^{m}} + \alpha_5(\beta\eta(r,s) + \mu_0)^m + \alpha_6(\beta\eta(r,s) + \mu_0)^{2m} + \alpha_7(\beta\eta(r,s) + \mu_0)^{3m} + \alpha_8(\beta\eta(r,s) + \mu_0)^{4m})$.

After linearizing the above expression (5.2) in β we obtain,

$$\iota\beta\eta_s + a\beta\eta_{rr} + \varpi\beta\eta = 0. \tag{5.3}$$

where $\varpi = (\frac{\alpha_1}{(\mu_0)^{4m}} + \frac{\alpha_2}{(\mu_0)^{3m}} + \frac{\alpha_3}{(\mu_0)^{2m}} + \frac{\alpha_4}{(\mu_0)^{m}} + \alpha_5(\mu_0)^m + \alpha_6(\mu_0)^{2m} + \alpha_7(\mu_0)^{3m} + \alpha_8(\mu_0)^{4m})$.

ϖ is the effective linear coefficient depending on μ_0 .Assume the solution of (5.3) is of the form,

$$\eta(r,s) = e^{\iota(\kappa r+\lambda s)}. \tag{5.4}$$

Where κ is normalized wave number, Insert (5.4) in expession (5.3) we obtain,

$$-\lambda - a\kappa^2 + \varpi = 0. \tag{5.5}$$

Solve the above expression (5.5) for λ, we obtain

$$\lambda = \varpi - a\kappa^2. \tag{5.6}$$

From expression (5.6) we can it is observed that the solution is stable when $\varpi < a\kappa^2$, and unstable when $\varpi > a\kappa^2$.

6 Physical interpretation

In the context of nonlinear optics, the new mapping analysis of generalized Kudryashov's equation GKE offers a rigorous mathematical framework for deriving precise analytical solutions, each of which has profound physical ramifications. The GKE simulates how an optical wave's phase is impacted by the intensity-dependent refractive index, resulting in a variety of phenomena such as collapse, soliton creation, and spectrum widening. Kink-type, periodic, bell, anti-bell, W shape and priodic are among the solutions obtained by suggested approach, each of which represents a distinct mode of nonlinear wave propagation. Figure 5 of $|Z_6(r,s)|$ Kink-type solutions, which physically correspond to nonlinear fronts or domain walls separating two stable intensity levels, are abrupt but continuous changes in the optical field profile.

These are especially important in optical systems that show bistability or switching behaviour, including fibre Bragg gratings and nonlinear directional couplers. They are perfect for optical memory or signal control applications because of their resilience, which is guaranteed by their topological stability.Figures 1,2 , 9 of $|Z_1(r,s)|$, $|Z_2(r,s)|$, $|Z_9(r,s)|$ represents modulated wave, W shape and periodic respectivel trains that move through a medium with steady periodicity are modelled by periodic solutions, which are represented by trigonometric, hyoerbolic or elliptic functions. Such structures are seen in nonlinear lattices [32], mode-locked lasers, and optical resonators, where quasi-periodic or harmonic wave patterns are formed by striking a balance between nonlinearity and dispersion.

In addition to being consistent with experimental findings of Bloch waves and discrete breathers in optical systems, these solutions are essential for comprehending phenomena such as modulation instability, a process that breaks apart continuous waves into pulse trains. At the other extreme, figures 3 peakon solutions of real part $Z_3(r,s)$ show blow-up behaviour, which means that the field amplitude diverges in limited space or time [33]. Despite being idealised, these singularities represent significant nonlinear effects that are frequently seen in high-intensity pulse propagation across Kerr media, including self-focusing, optical collapse, and laser filamentation. Higher-order phenomena like multiphoton absorption or saturable nonlinearity may regularise these singularities in real-world systems, but their existence in analytical solutions indicates crucial limits that classical propagation cannot cross. Such solutions' appearance emphasises how crucial nonlinear balancing and energy localisation are in optics.

All things considered, the solutions based on suggested approach a thorough mathematical explanation of the GKE as well as a clear correlation with behaviours seen in nonlinear optical systems through experimentation. These results align with well-established physics literature on optical wave propagation and soliton theory, as described in reputable publications such as Berge's. [34] review on wave collapse, Kivshar.[35] and Agrawal's. [36] Optical Solitons, and Agrawal's Nonlinear Fibre Optics. Moreover, the accurate solutions bridge analytical theory with contemporary photonic applications by advancing our understanding of wave modulation, pulse shaping, and optical turbulence.

7 Comparison

A nonlinear partial differential equation known as the generalized Kudryashov equation GKE is used to simulate the Kerr effect-induced nonlinear interaction of light in optical fibres. The equation's use in characterising wave dynamics in nonlinear media has garnered a lot of interest. The Kudryashov approach, the Tanh-Coth method, the exp-function method, and the Hirota bilinear method are among the many analytical techniques that have been implemented to provide exact answers to such nonlinear equations. This problem has been solved using the new mapping technique in this paper, and a comparison with alternative approaches shows some significant benefits and distinctions.

The modified simple equation approach's advantages are combined with better algebraic manipulation in the new mapping technique, a new analytical tool. This approach produces more general types of precise solutions, including brilliant solitons, kink-type,

periodic, bell, anti bell, peakon structures and exponentialÂ function solutions, when applied to the GKE problem. The New mapping method permits more expansive functional expressions, such as $sech$, tanh and their rational counterparts, in contrast to the Kudryashov method, which frequently results in particular rational or exponential forms. Because of its adaptability, a greater range of wave solutions may be investigated, many of which match physically meaningful situations in nonlinear optics. Another noteworthy advantage that has been mentioned is the flexibility in handling settings. By providing a natural framework for adding and maintaining arbitrary constants throughout the solution process, the novel mapping technique increases the flexibility of the solutions to meet real boundary circumstances. In contrast, methods like the tanh method and the exp-function approach often yield fixed-form solutions with little control over the amplitude and velocity parameters. Deriving parameterised families of solutions is made simpler by the novel mapping technique, which is useful for investigating the effects of nonlinearity, dispersion, and modulation depth. Furthermore, when applied to higher-order PDEs, the novel mapping methodology maintains its algebraic manageability, in contrast to methods like the exp-function or sub-equation method, which may require tedious algebra and may have issues with convergence or provide trivial solutions. It is therefore more trustworthy when examining both integrable and non-integrable versions of the GKE equation.

The findings of this study are consistent with previous studies by Wazwaz [37] and Kudryashov [38] that emphasised the need for generalised analytical techniques for nonlinear equations. The qualitative agreement between the solutions obtained in this work and those computed by Kumar and Malik [26] for other nonlinear models validates the validity and promise of the approach. In conclusion, the New mapping strategy offers a powerful alternative to traditional approaches for solving the GKE problem. Along with innovative and physiologically relevant solutions, it offers parameter freedom and computational simplicity. It is especially well-suited for in-depth studies of nonlinear wave propagation and optical soliton dynamics because of these features.

8 Conclusion

In this paper, we conducted an analytical investigation of the generalised Kudryashov equation, a nonlinear partial differential equation that properly mimics the propagation of ultra-short optical pulses in nonlinear and dispersive media.The model gives a more realistic portrayal of wave development in fibre optics and related physical systems by including higher-order nonlinear and dispersive phenomena. To investigate this intricate model, we developed

a novel generalised mapping technique. This approach transforms the nonlinear partial differential equation into a solved ordinary differential equation by a methodical transformation mechanism. strength of the proposed method lies in its universality and flexibility, since it is not reliant on the restricting solution forms commonly used in traditional approaches. With the use of this method, we were able to create a variety of precise soliton solutions, such as kink-type, brilliant, dark, and solitary wave solitons, each of which, depending on the model's parameter values, reflects a distinct physical phenomena.

These results show the effectiveness of the new mapping method in obtaining clear analytical solutions and its ability to handle complex nonlinear situations. The findings of this study contribute to the development of nonlinear wave theory and significantly enhance the framework for solving the generalised Kudryashov model. The range of soliton structures found demonstrates the complex dynamics of the model and the flexibility of the employed analytical technique. Future studies could extend this model by include stochastic effects like multiplicative or additive noise to emulate more realistic conditions with uncertainty. Moreover, further theoretical and practical advancements in the study of nonlinear wave propagation may arise from extending the mapping approach to other nonlinear equations and evaluating the stability of the resulting soliton profiles.

References

[1] Helal, M. A. (2002). Soliton solution of some nonlinear partial differential equations and its applications in fluid mechanics. *Chaos, Solitons & Fractals,* **13**(9), 1917-1929.

[2] Cheemaa, N., Seadawy, A. R., & Chen, S. (2019). Some new families of solitary wave solutions of the generalized Schamel equation and their applications in plasma physics. *The European Physical Journal Plus,* **134**(3), 117.

[3] Rosenfeld, J.S.: Developing flow-ecology relationships: implications of nonlinear biological responses for water management. *Freshw. Biol.* **62**(8), 1305â€“1324 (2017)

[4] Arshed, S., Biswas, A., Alzahrani, A. K., & Belic, M. R. (2020). Solitons in nonlinear directional couplers with optical metamaterials by first integral method. *Optik*, 218, 165208.

[5] Ablowitz, M. J., & Clarkson, P. A. (1991). Solitons, nonlinear evolution equations and inverse scattering (Vol. 149). *Cambridge university press.*

[6] Chow, K. W. (1995). A class of exact, periodic solutions of nonlinear envelope equations. *Journal of Mathematical Physics*, **36**(8), 4125-4137.

[7] Wazwaz, A. M. (2006). The modified decomposition method for analytic treatment of differential equations. *Applied mathematics and computation*, **173**(1), 165-176.

[8] Rezazadeh, H., Korkmaz, A., Eslami, M., Vahidi, J., & Asghari, R. (2018). Traveling wave solution of conformable fractional generalized reaction Duffing model by generalized projective Riccati equation method. *Optical and Quantum Electronics*, 50, 1-13.

[9] Liu, S., Fu, Z., Liu, S., & Zhao, Q. (2001). Jacobi elliptic function expansion method and periodic wave solutions of nonlinear wave equations. *Physics Letters A*, **289**(1-2), 69-74.

[10] Ahmed, H. M., Rabie, W. B., Arnous, A. H., & Wazwaz, A. M. (2020). Optical solitons in birefringent fibers of Kaup-Newell's equation with extended simplest equation method. *Physica Scripta*, **95**(11), 115214.

[11] Chow, K. W. (1995). A class of exact, periodic solutions of nonlinear envelope equations. *Journal of Mathematical Physics*,**36**(8), 4125-4137.

[12] Majid, S. Z., Faridi, W. A., Asjad, M. I., Abd El-Rahman, M., & Eldin, S. M. (2023). Explicit soliton structure formation for the riemann wave equation and a sensitive demonstration. *Fractal and Fractional*, **7**(2), 102.

[13] Asjad, M. I., Manzoor, M., Faridi, W. A., & Majid, S. Z. (2023). Precise invariant travelling wave soliton solutions of the Nizhnikâ€“Novikovâ€“Veselov equation with dynamic assessment. *Optik*, 294, 171438.

[14] Kaur, L., & Wazwaz, A. M. (2019). Lump, breather and solitary wave solutions to new reduced form of the generalized BKP equation. *International Journal of Numerical Methods for Heat & Fluid Flow*, **29**(2), 569-579.

[15] Sun, F. (2021). Optical wave patterns of nonlinear SchrÃ¶dinger equation with anti-cubic nonlinearity in optical fiber. *Results in Physics*, 31, 104889.

[16] Zayed, E. M., Alngar, M. E., Biswas, A., Asma, M., Ekici, M., Alzahrani, A. K., & Belic, M. R. (2020). Optical solitons and conservation laws with generalized Kudryashovâ€™s law of refractive index. *Chaos, Solitons & Fractals*, 139, 110284.

[17] Biswas, A., Ekici, M., Sonmezoglu, A., & Belic, M. (2019). Optical solitons in birefringent fibers with quadraticâ€“cubic nonlinearity by extended trial function scheme. *Optik*, 176, 542-548.

[18] Biswas, A., Ekici, M., Sonmezoglu, A., & Belic, M. R. (2019). Highly dispersive optical solitons with cubicâ€“quinticâ€“septic law by exp-expansion. *Optik*, 186, 321-325.

[19] Wazwaz, A. M., & Kaur, L. (2019). New integrable Boussinesq equations of distinct dimensions with diverse variety of soliton solutions. *Nonlinear Dynamics*, 97, 83-94.

[20] Sharif, A. (2021). New optical soliton solutions to the fractional hyperbolic nonlinear schrÃ¶dinger equation. *Advances in Mathematical Physics*, **2021**(1), 8484041.

[21] El-Shiekh, R. M., & Gaballah, M. (2020). Solitary wave solutions for the variable-coefficient coupled nonlinear SchrÃ¶dinger equations and Daveyâ€“Stewartson system using modified sine-Gordon equation method. *Journal of Ocean Engineering and Science*, **5**(2), 180-185.

[22] Aslan, E. C., & Inc, M. (2019). Optical soliton solutions of the NLSE with quadratic-cubic-Hamiltonian perturbations and modulation instability analysis. *Optik*, 196, 162661.

[23] Das, S., Dey, K. K., & Sekh, G. A. (2021). Optical solitons in saturable cubic-quintic nonlinear media with nonlinear dispersion. *Optik*, 247, 167865.

[24] El-Shiekh, R. M., & Gaballah, M. (2021). New rogon waves for the nonautonomous variable coefficients SchrÃ¶ dinger equation. *Optical and Quantum Electronics*, **53**(8), 431.

[25] Kaur, L., & Wazwaz, A. M. (2021). Einstein's vacuum field equation: PainlevÃ© analysis and Lie symmetries. *Waves in Random and Complex Media,* **31**(2), 199-206.

[26] Kumar, S., Kaur, L., & Niwas, M. (2021). Some exact invariant solutions and dynamical structures of multiple solitons for the (2+ 1)-dimensional Bogoyavlensky-Konopelchenko equation with variable coefficients using Lie symmetry analysis. *Chinese Journal of Physics,* 71, 518-538.

[27] Kudryashov, N. A. (2021). Implicit solitary waves for one of the generalized nonlinear SchrÃ¶dinger equations. *Mathematics,* **9**(23), 3024.

[28] Zayed, E. M., Alngar, M. E., Biswas, A., Asma, M., Ekici, M., Alzahrani, A. K., & Belic, M. R. (2020). Optical solitons and conservation laws with generalized Kudryashovâ€™s law of refractive index. *Chaos, Solitons & Fractals,* 139, 110284.

[29] Muniyappan, A., Hemamalini, D., Akila, E., Elakkiya, V., Anitha, S., Devadharshini, S., ... & Alshehri, H. M. (2022). Bright solitons with anti-cubic and generalized anti-cubic nonlinearities in an optical fiber. *Optik,* 254, 168612.

[30] Raza, N., Seadawy, A. R., Kaplan, M., & Butt, A. R. (2021). Symbolic computation and sensitivity analysis of nonlinear Kudryashovâ€™s dynamical equation with applications. *Physica Scripta,* **96**(10), 105216.

[31] Hussain, E., Mahmood, I., Shah, S. A. A., Khatoon, M., Az-Zoâ€™bi, E. A., & Ragab, A. E. (2024). The study of coherent structures of combined KdV-mKdV equation through integration schemes and stability analysis. *Optical and Quantum Electronics,* **56**(5), 723.

[32] Dudley, J. M., Genty, G., & Coen, S. (2006). Supercontinuum generation in photonic crystal fiber. *Reviews of modern physics*, **78**(4), 1135-1184.

[33] Karpman, V. I. (2016). Non-linear waves in dispersive media: *International series of monographs in natural philosophy* (Vol. 71). Elsevier.

[34] BergÃ©, L. (1998). Wave collapse in physics: principles and applications to light and plasma waves. *Physics reports*, **303**(5-6), 259-370.

[35] Kivshar, Y. S., & Agrawal, G. P. (2003). Optical solitons: from fibers to photonic crystals. *Academic press.*

[36] Agrawal, G. P. (2000). Nonlinear fiber optics. In Nonlinear Science at the Dawn of the 21st Century (pp. 195-211). Berlin, Heidelberg: *Springer Berlin Heidelberg.*

[37] Wazwaz, A. M. (2004). The tanh method for traveling wave solutions of nonlinear equations. *Applied mathematics and computation*, **154**(3), 713-723.

[38] Kudryashov, N. A. (1990). Exact solutions of the generalized Kuramoto-Sivashinsky equation. *Physics Letters A*, **147**(5-6), 287-291.